

Chandra observations of the accretion-driven millisecond X-ray pulsars XTE J0929–314 and XTE J1751–305 in quiescence

Rudy Wijnands¹, Jeroen Homan², Craig O. Heinke^{3,4,5} Jon M. Miller^{3,6}, Walter H. G. Lewin²

ABSTRACT

We observed the accretion-driven millisecond X-ray pulsars XTE J0929–314 and XTE J1751–305 in their quiescent states using *Chandra*. From XTE J0929–314 we detected 22 source photons (in the energy range 0.3–8 keV) in ~ 24.4 ksec, resulting in a background-corrected time-averaged count rate of $9 \pm 2 \times 10^{-4}$ counts s $^{-1}$. The small number of photons detected did not allow for a detailed spectral analysis of the quiescent spectrum, but we can demonstrate that the spectrum is harder than simple thermal emission which is what is usually presumed to arise from a cooling neutron star that has been heated during the outbursts. Assuming a power-law model for the time-averaged (averaged over the whole observation) X-ray spectrum, we obtain a power-law index of $1.8^{+0.6}_{-0.5}$ and an unabsorbed X-ray flux of $6^{+4}_{-2} \times 10^{-15}$ ergs s $^{-1}$ cm $^{-2}$ (for the energy range 0.5–10 keV), resulting in a 0.5–10 keV X-ray luminosity of $7^{+5}_{-2} \times 10^{31} (d/10 \text{ kpc})^2$ ergs s $^{-1}$, with d the distance toward the source in kpc. No thermal component could be detected; such a component contributed at most 30% to the 0.5–10 keV flux. Variability in the count rate of XTE J0929–314 was observed at the 95% confidence level. We did not conclusively detect XTE J1751–305 in our ~ 43 ksec observation, with 0.5–10 keV flux upper limits between 0.2 and 2.7×10^{-14} ergs s $^{-1}$ cm $^{-2}$ depending on assumed spectral shape, resulting in 0.5–10 keV luminosity upper

¹Astronomical Institute “Anton Pannekoek”, University of Amsterdam, Kruislaan 403, 1098 SJ, Amsterdam, the Netherlands; rudy@science.uva.nl

²Center for Space Research, Massachusetts Institute of Technology, 77 Massachusetts Avenue, Cambridge, MA 02139, USA; jeroen@space.mit.edu, lewin@space.mit.edu

³Harvard-Smithsonian Center for Astrophysics, 60 Garden Street, Cambridge, MA 02139, USA; cheinke@head.cfa.harvard.edu; jmmiller@head.cfa.harvard.edu

⁴Northwestern University, Dept. of Physics & Astronomy, 2145 Sheridan Rd., Evanston, IL 60208

⁵Lindheimer Postdoctoral Fellow

⁶NSF Astronomy & Astrophysics Fellow

limits of $0.2 - 2 \times 10^{32} (d/8 \text{ kpc})^2 \text{ ergs s}^{-1}$. We compare our results with those obtained for other neutron-star X-ray transients in their quiescent state, and in particular with the quiescent properties of SAX J1808.4–3658. Using simple accretion disk physics in combination with our measured quiescent luminosity of XTE J0929–314 and the luminosity upper limits of XTE J1751–305, and the known spin frequency of the neutron stars, we could constrain the magnetic field of the neutron stars in XTE J0929–314 and XTE J1751–305 to be less than $3 \times 10^9 \frac{d}{10 \text{ kpc}}$ and $3 - 7 \times 10^8 \frac{d}{8 \text{ kpc}}$ Gauss (depending on assumed spectral shape of the quiescent spectrum), respectively.

Subject headings: accretion, accretion disks — stars: neutron stars: individual (XTE J0929–314; XTE J1751–305)— X-rays: stars

1. Introduction

Neutron stars in low-mass X-ray binaries accrete matter from solar mass companion stars. The sub-group of neutron-star transients spend most of their time in quiescence during which hardly any or no accretion occurs onto their neutron stars. However, these transients sporadically become very luminous in X-rays ($>10^{36-38} \text{ ergs s}^{-1}$) owing to a huge increase in the accretion rate. During those outbursts, these sources can be readily studied with the available X-ray instruments, but so far only about a dozen sources have been studied in their much dimmer quiescent states. In quiescence, they typically exhibit 0.5–10 keV luminosities of $10^{32-34} \text{ ergs s}^{-1}$ and their spectra are usually dominated by a soft component which can be described by a thermal model (either a black-body or a neutron-star atmosphere model). This emission is generally ascribed to the cooling of the neutron star which has been heated during the outbursts (e.g., via deep crustal heating; Brown, Bildsten, & Rutledge 1998). For several quiescent systems an additional power-law shaped component is present in their X-ray spectra and it dominates above a few keV (e.g., Asai et al. 1998; Rutledge et al. 2001). The origin of this power-law component is not understood but it has been proposed to be due to residual accretion on the neutron-star magnetic field, an active pulsar mechanism, or shock emission due to the interaction of the pulsar wind and matter which is still being transferred from the companion star (e.g., Stella et al. 1994; Campana et al. 1998; Campana & Stella 2000).

The fractional contribution of this power-law component to the flux in the 0.5–10 keV energy range varies significantly between systems. In some systems this component cannot be detected (with less than 10% of the 0.5–10 keV flux possibly due to such a component), but in other systems it contributes up to half the emission in the 0.5–10 keV energy range

(e.g., Asai et al. 1998; Rutledge et al. 2001). Currently, only two quiescent systems (SAX J1808.4–3658 and EXO 1745–248) have been found to exhibit quiescent spectra which are fully dominated by the power-law component (with over 90% of the 0.5–10 keV flux due to the power-law component; Campana et al. 2002; Wijnands et al. 2004). For several other systems (i.e., SAX J1810.8–2609 and XTE J2123–058; Jonker, Wijnands, & van der Klis 2004a; Tomsick et al. 2004) it has also been found that the quiescent spectra could be adequately fitted with only a power-law model. However, the statistics of the data for those sources were rather limited, still allowing for a thermal component which contributed more than 50%–70% to the 0.5–10 keV flux.

During outburst SAX J1808.4–3658 is an accretion-driven millisecond X-ray pulsar and its anomalous X-ray properties in quiescence (its hard quiescent spectrum and low luminosity of $\sim 5 \times 10^{31}$ ergs s $^{-1}$; Campana et al. 2002) might be related to the expected higher magnetic field strength of the neutron star in this system, compared to that of the neutron stars in the non-pulsating systems. However, the recent study of the neutron-star X-ray transient EXO 1745–248 located in the globular cluster Terzan 5 during its quiescent state has cast doubt on this hypothesis. Wijnands et al. (2004) found that the Terzan 5 system, which is not observed to pulsate during outburst, also had a quiescent spectrum which was fully dominated by the power-law component (more than 90% of the 0.5–10 keV flux was due to the power-law component) just like SAX J1808.4–3658. However, EXO 1745–248 had a quiescent luminosity ($\sim 2 \times 10^{33}$ ergs s $^{-1}$) which was a factor of ~ 40 higher than what has been observed for SAX J1808.4–3658.

The physical process(es) behind the power-law component and the differences among sources in terms of the properties of this spectral component are unknown. However, some clues about the nature of this spectral component were recently glimpsed in the work by Jonker et al. (2004a, b). They compared all quiescent neutron star X-ray transients for which spectral information was available and found that the fractional contribution of the power-law component to the 0.5–10 keV fluxes is lowest when these sources have quiescent luminosities of $\sim 1 - 2 \times 10^{33}$ ergs s $^{-1}$. They found that both at higher and lower quiescent luminosities the fractional contribution of the power-law component to the 0.5–10 keV flux increases. So far, only EXO 1745–248 did not follow this correlation. It remains to be seen whether this transient is an unusual system or if the correlation found by Jonker et al. (2004a, b) is spurious and more sources similar to EXO 1745–248 will be found.

In recent years, four additional accreting millisecond X-ray pulsars (after SAX J1808.4–3658) have been discovered (Markwardt et al. 2002; Galloway et al. 2002; Markwardt, Smith, & Swank 2003; Markwardt & Swank 2003). Those systems are prime targets to observe in quiescence to test the hypothesis that the unusual quiescent properties of SAX J1808.4–3658

are due to a relatively strong neutron-star magnetic field strength compared to that of the non-pulsating systems: one would expect that the magnetic fields of the neutron stars in those additional systems are of similar strength as that of the neutron star in SAX J1808.4–3658. To this end we had observations of XTE J1751–305 and XTE J0929–314 scheduled during cycle 5 of *Chandra*. Here we report on the results of those observations.

The second accretion driven millisecond X-ray pulsar, XTE J1751–305, was discovered on April 3, 2002 (Markwardt et al. 2002). It was found to harbor a neutron star with a spin frequency of 435 Hz which is located in a binary system with an orbital period of 42 minutes (Markwardt et al. 2002). The third accreting millisecond X-ray pulsar, XTE J0929–314, was discovered by Remillard (2002) on April 13–18, 2002, using the all-sky monitor (ASM) aboard the *Rossi X-ray Timing Explorer* (*RXTE*). Only later (May 2, 2002), when the proportional counter array aboard *RXTE* observed the source, was it discovered to be an accreting millisecond X-ray pulsar with a pulse frequency of 185 Hz (Remillard, Swank, & Strohmayer 2002). The orbital period of the system was found to be 44 minutes (Galloway et al. 2002).

2. Observations, analysis, and results

We observed XTE J0929–314 with *Chandra* on March 18, 2004, between 02:30 and 10:02 UT (resulting in an exposure time of \sim 24.4 ksec) and XTE J1751–305 on June 26, 2004 between 07:59 and 21:12 UT (resulting in an exposure time of \sim 43.0 ksec). We used the ACIS-S3 CCD and we selected a 1/4 sub-array to limit the pile-up in case the source fluxes exceeded \sim 10^{−12} ergs s^{−1} cm^{−2} (as we will show below, both sources had quiescent fluxes significantly lower than this flux level so no pile-up occurred during our observations). We checked for background flares during our observations, but none were found allowing us to use all available data. Our analyzes were performed using the CIAO software package (version 3.1) and the standard *Chandra* analysis threads¹.

¹See <http://cxc.harvard.edu/ciao/> for CIAO and the analysis threads

2.1. XTE J0929–314

2.1.1. Image analysis

We used the tool 'wavdetect' to search for point sources in our data of XTE J0929–314 and to obtain the coordinates of each source which was detected. For XTE J0929–314, we used the tool 'dmextract' to extract the number of observed photons and the count rate (for the energy range 0.3–8 keV). As source extraction region we used a circle centered on the source position (as obtained with 'wavdetect') with a radius of 1.5''. For background extraction region we used an annulus centered on the source position with an inner radius of 5'' and an outer radius of 20'' (a larger outer radius could not be used since the field source CXOU J092919.1–312244 was within 25'' of XTE J0929–314 as can be seen in Fig. 1 left panel). We detected four sources in our image, including XTE J0929–314; we will not discuss the other three sources further in this article. Instead we concentrate on the observed X-ray properties of XTE J0929–314 in its quiescent state. The coordinates we obtained for XTE J0929–314 are right ascension $09^h 29^m 20^s.180$ and declination $-31^\circ 23' 03''.5$ (epoch J2000.0), which are consistent with the coordinates of the source obtained during outbursts in the X-ray (Juett, Galloway, & Chakrabarty 2003), optical (Greenhill, Giles, & Hill 2002), and radio bands (Rupen, Dhawan, & Mioduszewski 2002; see Fig. 1 right panel). The total number of source photons detected in the energy range 0.3–8 keV from XTE J0929–314 is 22, resulting in a net time-averaged count rate of $9 \pm 2 \times 10^{-4}$ counts s $^{-1}$ (after background subtraction; less than 0.4 background photons are expected in our source extraction region).

2.1.2. Count rate analysis

In Figure 2 we plot the energies of the X-ray photons (0.3–8 keV energy range) detected at the source position against the arrival time of the photons (measured since the start of the observation). From this figure it can be seen that 4 photons are detected with energies above 3 keV (note that no photons were detected with energies >5 keV) and the remainder of the photons have energies below ~ 2.5 keV. In the last ~ 10 ksec of the observation only two source photons are detected compared with twenty photons during the first ~ 15 ksec; this might suggest that the source exhibited variability during our observation. To investigate if XTE J0929–314 was indeed variable during our observation, we applied Kolmogorov-Smirnov and Cramer-Von Mises tests on the event list (as shown in Figure 2) to attempt to disprove the hypothesis that the source count rate is constant. Both tests showed that XTE J0929–314 is variable for energies between 0.3 and 8 keV (although effectively only up to 5 keV since no photons are detected above that energy) at the 95% confidence level. From Figure 2 it can

be seen that the four photons which have energies >3 keV all arrived within the first 5000 seconds of the observation, which may be the main cause of the variability detected in the source. Therefore, we also applied the above two tests to the event list for photon energies between 0.3 and 2.5 keV. The Kolmogorov-Smirnov test revealed that the 0.3–2.5 keV event list might also be variable but only at a 90% confidence level. The Cramer-Von Mises test could not find evidence for variability in this energy range. Therefore, we conclude that the variability observed in the source is likely stronger at higher photon energies.

2.1.3. Time-averaged X-ray spectrum

Despite the low number of photons detected, we extracted the source spectra (averaged over the whole duration of the observation) using the CIAO tool 'psextract' for the energy range 0.3–8 keV, which also created the response matrix and the ancillary response files (the latter was also automatically corrected for the time-variable low-energy quantum efficiency degradation of the CCD). We used a circle with a radius of $1.5''$ as source extraction region. We fitted the spectrum using Xspec version 11.3.0 (Arnaud 1996). The small number of photons observed does not allow for χ^2 statistics to be used during the fits. Therefore, we fitted the data using Cash statistics (Cash 1979). Since Cash statistics cannot be used on background subtracted spectra, we did not subtract the background from our data. The errors thus introduced are likely to be small since less than 0.4 background photons are expected in the source extraction region (see above). The quality of the fits was investigated by generating 10,000 Monte Carlo simulations of the best-fit spectrum: if the fit is good, roughly half the simulations should have values of the Cash statistics which are lower than those of the data.

In all our spectral fits we left the interstellar column density N_{H} as a free parameter. To calculate the errors on the obtained fluxes, we fixed each free fit parameter one at a time, either to its minimum or maximum allowed value as obtained from the fits. After that we refitted the data and recalculated the fluxes. This process was then repeated for each free parameter and the final flux range determined the flux errors. The spectra of neutron-star X-ray transients in their quiescent states are usually dominated by a soft thermal component which can adequately be fitted with a neutron-star hydrogen atmosphere model for non-magnetized stars (the NSA model; we used that of Zavlin, Pavlov, & Shibanov 1996; we also assumed a mass of $1.4 M_{\odot}$ and a radius of 10 km for the neutron star in XTE J0929–314). In such a model the normalization is given by $\frac{1}{d^2}$, with d the distance to the source in parsecs. The distance toward XTE J0929–314 is not known but it is constrained to be >5 kpc (Galloway et al. 2002). When leaving the normalization free, 88% of the simulated spectra

have better Cash-statistics than the data demonstrating that this model does not provide an accurate description of the data (Fig. 3 *bottom*). From this model we obtained an effective temperature kT_∞ (for an observer at infinity) of 0.3 ± 0.1 keV and the column density is $< 3 \times 10^{20}$ cm $^{-2}$. However, the normalization was constrained to be $< 1 \times 10^{-11}$, resulting in a distance constrain of > 316 Mpc. This unrealistic distance limit further demonstrates that a simple NSA model does not provide a good fit to the data.

We also fitted the data using the NSA model but with the normalization fixed and assuming three distances: 5, 10, or 15 kpc. The results are listed in Table 1 and shown in Figure 3 (top). From this table it can be seen that such a model does not provide an acceptable fit to the data since 100% of the simulated spectra have lower values for the Cash-statistics than the data themselves. We also fitted a simple blackbody model to the data but again such a model did not provide an adequate fit to the data with a fit quality of 0.94 and a kT of $0.6^{+0.2}_{-0.1}$ keV (and $N_H < 3 \times 10^{20}$ cm $^{-2}$). The radius of the emitting area was $< 0.12 \times \frac{d}{10 \text{ kpc}}$ km, with d the distance in kpc, much smaller than the expected radius of a neutron star. The inability of the thermal models to provide an adequate fit to the data and the fact that four photons are detected with energies above 3 keV point to a X-ray spectrum which is significantly harder than a simple thermal model. Therefore, we fitted the X-ray spectrum with a power-law model (Fig. 3; Tab. 1). The fit quality of 0.68 using such a model is considerably better than for a thermal model (0.68 versus > 0.88). The fit resulted in a power-law photon index Γ of $1.8^{+0.6}_{-0.5}$, a column density of $< 6 \times 10^{20}$ cm $^{-2}$, and a 0.5–10 keV flux of $6^{+4}_{-2} \times 10^{-15}$ ergs s $^{-1}$ cm $^{-2}$ (corrected for absorption). This gives an unabsorbed 0.5–10 keV X-ray luminosity of $7^{+5}_{-2} \times 10^{31} (\frac{d}{10 \text{ kpc}})^2$ ergs s $^{-1}$, with d the distance in kpc.

To obtain limits on the temperature and luminosity of a possible thermal component in the data, we fitted the spectrum with a power-law component plus a neutron-star atmosphere component. We again fixed the normalization of the neutron-star atmosphere component to correspond to 5, 10, or 15 kpc but left the other parameters free (i.e., the column density, the effective temperature, the photon index, and the normalization of the power-law component). The maximum allowed temperatures and bolometric luminosities are listed in Table 2, together with the minimum fraction of the 0.5–10 keV flux which is due to the power-law component. The table shows that the maximum allowed kT_∞ is between 0.04 and 0.05 keV with a corresponding maximum allowed bolometric luminosity of $0.4 - 1.7 \times 10^{32}$ ergs s $^{-1}$ (for both parameters the highest values are obtained for the cases which assume the largest distance). For all assumed distances, at least $\sim 70\%$ of the flux in the 0.5–10 keV range is due to the power-law component. This demonstrates that the power-law component dominates the X-ray emission in the range 0.5–10 keV for XTE J0929–314.

2.1.4. Spectral variability

In § 2.1.2 we demonstrated that XTE J0929–314 exhibited variability in its count rate at the 95% confidence level. It is possible that this count rate variability is accompanied by or even due to changes in the X-ray spectrum of the source. If true, the spectral results we obtained in § 2.1.3 only represent a time-averaged view of the spectral properties of the source. To investigate if indeed XTE J0929–314 exhibited spectral variability we calculated X-ray hardness ratios from the first part of the observation (between 0 and 10 ksec after the start of the observation; 13 photons were detected in this time interval) and the second part of the observation (the remaining \sim 14 ksec of the observation; 9 photons were detected). As X-ray hardness ratio we used the logarithm of the ratio between the number of photons detected with energies >1 keV and the number of photons detected with energies <1 keV. In Figure 4 (*top panel*) we show the hardness ratio versus time. During the second part of the observation the hardness ratio is smaller than during the first part, but the error bars are large and the data are consistent with a non-variable spectrum.

Hong, Schlegel, & Grindlay (2004) have argued that the X-ray hardness ratios normally used in the literature (e.g., those we used in the previous paragraph) are not appropriate for sources with low numbers of counts. Since we have roughly 10 counts to construct our hardness ratios, these ratios might not represent an accurate description of the spectral shape of XTE J0929–314. Therefore, we also calculate so-called “quantiles” using the quantile method outlined by Hong et al. (2004)². Hong et al. (2004) found that the quantity $\log_{10} \frac{Q_{50}}{1-Q_{50}}$, with Q_{50} the median quantile, provided a good indication for the spectral hardness of a source. Therefore, in the bottom panel of Figure 4 we plot this quantity as a function of time. Similar to the hardness ratios, the error bars on the quantiles are such that a constant spectral shape throughout the observation cannot be excluded.

As a last way of investigating possible spectral variability, we extracted the X-ray spectrum for each of the two time intervals used above. The results of the spectral fitting are listed in Table 3. When fitting the two data sets separately, a power-law model produces acceptable fits (with fit quality of 0.6–0.7) with photon indices of $1.3^{+0.9}_{-0.7}$ and $2.6^{+1.2}_{-0.9}$ for the first and second part of the observation, respectively. The values again indicate that the source spectrum had softened during the course of the observation, although the indices are consistent with each other (within the errors). The 0.5–10 keV X-ray flux decreased

²The errors on the quantiles were calculated using the method of Maritz & Jarret (1978; see Hong et al. 2004) but Hong et al. (2004) demonstrated, using simulations, that the errors on the quantiles are overestimated when the source counts are very low, as in our case. Therefore, we corrected the quantile errors using the corrections provided by Hong et al. (2004).

by a factor of 3–4 during the observation indeed suggesting variability in the brightness of the source (note, again the errors are large and only minimal variability might have been present). To further investigate how significant the softening of the X-ray spectrum is, we fitted the two data sets simultaneously. During this fit, we assumed that the column density did not vary during the observation and we tied it between the two data sets. The fit results were consistent with those obtained when fitting the data sets separately (Tab. 3). In Figure 5 we plot the confidence regions of the photon indices, showing that the two indices are only different from each other at the <90% confidence level. This is illustrated in the figure by the line of equal index between two data sets which intersects the 90% confidence contour. We conclude that the limited statistics does not allow for any strong conclusions on the possible softening of the X-ray spectrum suggested by Figure 2.

We investigated if a thermal model could fit the two data sets, but when using a NSA model with fixed normalization (to a distance of 5, 10, or 15 kpc), the fit qualities were always 1.00 for the first part of the observation and between 0.89 and 0.94 (larger for smaller assumed distance) for the second part of the observation. Also a simple black-body model does not produce a good fit with fit qualities of 0.85 and 0.87 for the first and second part of the observation, respectively. This clearly demonstrates that during the whole observation, the source had an X-ray spectral shape which was significantly different (i.e., harder) from a simple thermal model. This confirms our conclusions in § 2.1.3. Investigations into whether or not the fractional contribution of the power-law component to the 0.5–10 keV flux changed during the observation did not result in useful insights due to the limitation on the statistics of the individual data sets.

2.2. XTE J1751–305

We begin a similar analysis for XTE J1751–305 by searching for point sources in our data (using ‘wavdetect’). We detected 34 sources in our image but XTE J1751–305 itself was not detected (a discussion of the properties of these 34 sources, unrelated to XTE J1751–305, is beyond the scope of this article). In Figure 6 we show the 0.5–7 keV X-ray image near the position of XTE J1751–305. Several point sources are detected close to the position of XTE J1751–305 (obtained during outburst using *Chandra*; Markwardt et al. 2002), but only 1 photon was detected (in the energy range 0.5–7 keV) in a circle with a radius of 1" around the position of XTE J1751–305 (for *Chandra*’s point-spread-function, 1" corresponds to the encirclement of 90% of the energy), which does not constitute a significant detection. When using also the data at lower energies (i.e., using the energy range 0.3–7.0 keV), we still could only detect 2 photons within an 1" radius. When using a larger radius of 1.5", 3 photons

are detected for the energy range 0.5–7 keV, and 5 photons for the energy range 0.3–7 keV. However, in these cases more than half the possible source photons would fall outside the circle which should encircle >90% of the energy, which is unlikely. Moreover, the positions of the two softest photons (those with energies <0.45 keV) were consistent with the position of a bright *K* star close to the position of XTE J1751–305 (1.2" away; the two photons have a distance of 0.5" and 0.8" from the position of this star). Thus these two photons could have possibly originated from this star and not from XTE J1751–305, especially because the high column density toward the pulsar ($\sim 10^{22}$ cm $^{-2}$; Miller et al. 2003) would make unlikely any detection of its photons which have energies below 0.5 keV.

The closest, significantly detected X-ray source (the one to the south-east of XTE J1751–305) is located 3.8" away³ from XTE J1751–305. The absolute positional accuracy of *Chandra* is 0.6" (90% confidence level; 0.8" for 99% confidence level⁴) strongly suggesting that this south-east source is not the quiescent counterpart of XTE J1751–305. It might be possible that during our observation the positional accuracy of *Chandra* was (for some reason) extremely inaccurate. To test this hypothesis, we compared our X-ray image with the *K*-band image of the region around XTE J1751–305 published by Jonker et al. (2003). Of the 13 X-ray sources located in the region covered by this *K*-band image, 8 have *K* objects located within a radius of 0.6" (including the X-ray source located 3.8" away from XTE J1751–305 as well as the four other reasonably bright X-ray point sources visible in Fig. 6). We simulated 10,000 X-ray point sources with random positions in the field of the *K* image. Only <7% of the simulated sources have a *K* star (of similar or higher brightness than the potential *K* counterparts of the detected X-ray point sources) falling within a 0.6" radius of their positions. The coincidence rate between the detected X-ray sources and the *K* stars is significantly higher ($\sim 60\%$) than the simulated one demonstrating that most of the *K* stars located in the X-ray error circles are indeed the infrared counterparts of those X-ray sources. Our analysis strongly suggests that the positional accuracy of our X-ray image is within the standard accuracy quoted for *Chandra*. Therefore, we conclude that XTE J1751–305 was not conclusively detected during our *Chandra* observation.

To calculate a flux upper limit for XTE J1751–305, we assume that <5 photons⁵ (for the energy range 0.5–7 keV) were detected from the source, resulting in a count rate upper

³The coordinates of this source are: right ascension $17^h 51^m 13^s.673$, declination $-30^\circ 37' 26''.40$. The coordinates are for epoch J2000.0 and have errors of 0.6" (90% confidence levels).

⁴See <http://cxc.harvard.edu/cal/ASPECT/celmon/>

⁵Using 5 photons as an upper limit can be interpreted (Gehrels 1986) as a 97% or 90% confidence upper limit for 1 or 2 detected photons from the source, respectively, which is the number of photons we possible detected from XTE J1751–305.

limit of 1.16×10^{-4} counts s^{-1} (0.5–7 keV). We used PIMMS⁶ to calculate the flux upper limits assuming different spectral model. As column density we used the value as observed during outburst ($N_{\text{H}} = 9.8 \times 10^{21} \text{ cm}^{-2}$; Miller et al. 2003) and we assume a black-body spectral shape⁷ (with temperatures kT of 0.05–0.7 keV) or a power-law spectral shape (with a photon index Γ of 0–4). Using a black-body model, we find that the 0.5–10 keV flux upper limit F_{upper} (in units of $\text{ergs s}^{-1} \text{ cm}^{-2}$) can be accurately approximated by

$$\log_{10} F_{\text{upper}} = -14.787 + 4.09e^{-\frac{kT}{0.0827 \text{ keV}}} \quad (1)$$

Using a power-law model, we find

$$F_{\text{upper}} = 5.76 \times 10^{-15} - 3.05 \times 10^{-15}\Gamma + 7.41 \times 10^{-16}\Gamma^2 \quad (2)$$

For a reasonable range in kT of 0.1–0.3 keV (as observed in other quiescent neutron star X-ray transients), we find 0.5–10 keV upper limits of $0.2 - 2.7 \times 10^{-14} \text{ ergs s}^{-1} \text{ cm}^{-2}$ (the highest upper limits are obtained when the assumed kT is smallest). For a reasonable Γ of 1–3, the 0.5–10 keV flux upper limit is $2.6 - 3.5 \times 10^{-15} \text{ ergs s}^{-1} \text{ cm}^{-2}$ (the minimum upper limit is obtained when $\Gamma \sim 2$).

3. Discussion

We have observed the accretion-driven millisecond X-ray pulsars XTE J0929–314 and XTE J1751–305 in their quiescent states. This triples the number of such sources to be observed in their quiescent states (the first one being SAX J1808.4–3658; Stella et al. 2000; Dotani, Asai, & Wijnands 2000; Campana et al. 2002). We could not detect XTE J1751–305 during our observations, which resulted in upper limits on the quiescent X-ray flux (0.5–10 keV; corrected for absorption) of this system of $2.6 - 3.5 \times 10^{-15} \text{ ergs s}^{-1} \text{ cm}^{-2}$ when we assume that the source exhibited a power-law spectral shape with photon index between 1 and 3, or $0.2 - 2.7 \times 10^{-14} \text{ ergs s}^{-1} \text{ cm}^{-2}$ when assuming a black-body spectral shape with kT of 0.1–0.3 keV. We conclusively detected XTE J0929–314, but we detected only 22 photons (energy range 0.3–8 keV) during our observation which limits any detailed analysis. The

⁶Available <http://heasarc.gsfc.nasa.gov/Tools/w3pimms.html>

⁷Although a neutron-star atmosphere model is usually fitted to the X-ray spectra of quiescent neutron star X-ray transients, such a model cannot be used in PIMMS and we had to resort to the black-body model as an approximation.

X-ray spectrum could not be fitted with a simple thermal model alone (such as a black-body or a neutron-star atmosphere model) but a single power-law model provided an adequate fit to the data resulting in a 0.5–10 keV X-ray luminosity of $7_{-2}^{+5} \times 10^{31} (\frac{d}{10 \text{ kpc}})^2$ ergs s^{−1} (with d in kpc). The upper limits on the effective temperature of a thermal component ranged from 0.04 to 0.05 keV with corresponding upper limits on the bolometric luminosity of $0.4\text{--}1.7 \times 10^{32}$ ergs s^{−1} (both quantities are for an observer at infinity). We determined that at most $\sim 30\%$ of the 0.5–10 keV flux could have come from such a thermal component. We could demonstrate that the source was variable at the 95% confidence level but, within the limitation of the statistics, we could not find evidence for spectral variability during our observation. Next, we will first discuss what can be inferred from the results of XTE J0929–314 before we discuss the non-detection of XTE J1751–305.

3.1. The power-law component of XTE J0929–314

Our results suggest that the X-ray emission of XTE J0929–314 in its quiescent state is dominated by a power-law component and not by a thermal component as is usually observed during the quiescent states of neutron-star X-ray transients. This makes XTE J0929–314 similar to SAX J1808.4–3658, which was until now the only accreting millisecond pulsar to have been observed in its quiescent state. In quiescence, SAX J1808.4–3658 was found to have a 0.5–10 keV X-ray luminosity of $\sim 5 \times 10^{31}$ ergs s^{−1} when fitted with a power-law model with index of 1.5 ± 0.3 (Campana et al. 2002). This is rather similar to the 0.5–10 keV luminosity ($\sim 7 \times 10^{31}$ ergs s^{−1} for a distance of 10 kpc) and power-law index ($1.8_{-0.5}^{+0.6}$) of XTE J0929–314. Furthermore, the quiescent X-ray emission between 0.5 and 10 keV was in both sources dominated by the power-law component ($>90\%$ in SAX J1808.4–3658 and $>70\%$ in XTE J0929–314). Although our statistics on the XTE J0929–314 data are poor, the only difference between the two sources seems to be that SAX J1808.4–3658 has a somewhat lower luminosity in quiescence and perhaps a bit harder spectrum. We note that the errors on the parameters also suggest that both sources could have equal luminosities and spectral hardness. Furthermore, XTE J0929–314 exhibited luminosity variability during our observation possibly accompanied by (or even due to) spectral variability. This means that XTE J0929–314 could be at times intrinsically fainter than SAX J1808.4–3658 or have a harder spectrum (note that it is less likely that XTE J0929–314 was fainter *and* harder than SAX J1808.4–3658, since the indication is that the hardest spectrum was observed when XTE J0929–314 was brightest).

The results on XTE J0929–314 and SAX J1808.4–3658 might suggest that a power-law dominated X-ray spectrum in quiescence and a low quiescent 0.5–10 keV luminosity

are common properties of accretion-driven millisecond X-ray pulsars. However, recent work (as discussed below) on two other weak quiescent neutron-star X-ray transients, which do not exhibit pulsations, suggests that this might instead be a property of many weak quiescent neutron-star X-ray transients in general and not only of the accreting millisecond X-ray pulsars. Jonker et al. (2004a) and Tomsick et al. (2004) reported on quiescent X-ray observations of SAX J1810.8–2609 and XTE J2123–058, respectively. For both sources it was found that their quiescent X-ray spectra could be fitted with a power-law model with indices of ~ 3 and an 0.5–10 keV X-ray luminosity around $\sim 10^{32}$ ergs s $^{-1}$. No thermal component could be detected with a maximum contribution to the 0.5–10 keV flux of $\sim 50\%$ in SAX J1810.8–2609 (Jonker et al. 2004a) and $\sim 60\%$ – 70% in XTE J2123–058 (Tomsick et al. 2004). These luminosities are somewhat higher than those of SAX J1808.4–3658 and XTE J0929–314 and the X-ray spectra somewhat softer, but they are among the lowest luminosity quiescent neutron-star X-ray transients for which no X-ray pulsations were seen during their outbursts.

Jonker et al. (2004a, b) used the results obtained for SAX J1808.4–3658, SAX J1810.8–2609, and XTE J2123–058 together with those obtained for the other quiescent neutron star X-ray transients, to show evidence that, in their quiescent spectra, the contributions of the power-law components to the 0.5–10 keV flux seem to increase (from at most several tens of percents to over 90%) when the quiescent source luminosities decrease from $\sim 10^{33}$ ergs s $^{-1}$ to approximately 5×10^{31} ergs s $^{-1}$. They also found a similar trend for higher quiescent luminosities of the transients: the fractional power-law contribution also increases when the quiescent source luminosities increase from the comparison luminosity of 1 – 2×10^{33} ergs s $^{-1}$. Our results show that XTE J0929–314 fits between SAX J1808.4–3658 on the low-luminosity side, and SAX J1810.8–2609 and XTE J2123–058 on the higher-luminosity side, which provides additional support to the possible correlations found by Jonker et al. (2004a, b). This result would suggest that hard quiescent emission is not a feature unique to accretion-driven millisecond X-ray pulsars but rather a general feature of quiescent neutron-star X-ray transients when they are at low quiescent luminosities (with increasingly harder spectra when the luminosities get lower). The current data still suggest that the accretion-driven millisecond X-ray pulsars might have slightly lower luminosities and harder spectra than the other sources, but it remains to be seen if this holds when additional neutron-star X-ray transients are observed in their quiescent states. Additional neutron star X-ray transients need to be studied in their quiescent states to better understand the power-law spectral component in the quiescent spectra. Such studies might also clarify if the quiescent transient in Terzan 5 (EXO 1745–248; Wijnands et al. 2004), which does not follow this correlation (Jonker et al. 2004b), is unique among the quiescent neutron star systems, or if it is the first example of many similar systems which would suggest that this correlation is spurious.

3.2. The non-detection of a thermal component in XTE J0929–314

We can investigate whether our upper limits on the contribution of the thermal component to the quiescent spectrum of XTE J0929–314 are consistent with what would be expected from the cooling neutron star model proposed by Brown et al. (1998). The quiescent thermal luminosity predicted by this model depends on the time-averaged (over $>10,000$ years) accretion rate of the source. For XTE J0929–314 we can estimate its time-averaged accretion rate in two ways; either by using the outburst fluence of the source and the limited information about the outburst recurrence time, or by assuming that the mass transfer is solely due to gravitational radiation and all matter is eventually accreted onto the neutron star.

3.2.1. Constraints obtained when using the 2002 outburst fluence

According to Galloway et al. (2002), the 2–60 keV fluence of the 2002 outburst of XTE J0929–314 was 4.2×10^{-3} ergs cm $^{-2}$, with an estimated bolometric correction of ~ 2.34 . This results in a bolometric fluence of $\sim 9.8 \times 10^{-3}$ ergs cm $^{-2}$. During the lifetime of *RXTE* (which is at present 8.5 years), only 1 outburst has been observed, resulting in a time averaged accretion flux $\langle F_{\text{acc}} \rangle$ of $< 3.7 \times 10^{-11}$ ergs s $^{-1}$ cm $^{-2}$. Using the Brown et al. (1998) model and assuming standard core cooling, the expected quiescent flux F_q is approximately given by $F_q = \frac{\langle F_{\text{acc}} \rangle}{135}$ (Brown et al. 1998; Wijnands et al. 2001; Rutledge et al. 2002). For XTE J0929–314, this results in $F_q < 2.7 \times 10^{-13}$ ergs s $^{-1}$ cm $^{-2}$, which is consistent with the upper limits on the bolometric fluxes of a possible neutron-star atmosphere component in the quiescent spectra (which are $< 1.5 \times 10^{-14}$ ergs s $^{-1}$ cm $^{-2}$). However, in this scenario the source would have to remain quiescent for a significant period (i.e., much longer than the 8.5 years we assumed here) to allow the predicted limits to come down to the measured flux limits.

Using our measured flux limits, we can actually estimate how long XTE J0929–314 has to be in quiescence for the neutron star surface to be as cool as we measure if the neutron star cools down using standard core cooling processes. From $F_q = \frac{\langle F_{\text{acc}} \rangle}{135}$ it can be derived (Wijnands et al. 2001) that $F_q \approx \frac{t_o}{t_o + t_q} \times \frac{\langle F_o \rangle}{135}$, with $\langle F_o \rangle$ the averaged flux during outburst, t_o the averaged time the source is in outburst, and t_q the averaged time the source is in quiescence. From Galloway et al. (2002), it follows that $t_o \approx 73$ days (if the 2002 outburst had a duration which is typical for the source) and $\langle F_o \rangle = 1.6 \times 10^{-9}$ ergs s $^{-1}$ cm $^{-2}$. Using our limits on $F_q < 1.5 \times 10^{-14}$ ergs s $^{-1}$ cm $^{-2}$, then $t_q > 5.8 \times 10^4$ days, resulting in $t_q > 160$ years. Although this predicted quiescent period is quite long compared to the known recurrence time of several other neutron-star X-ray transients (ranging from

less than 1 year up to several decades; e.g., Chen, Shrader, & Livio 1997), the disk instability model proposed for the outburst behavior of X-ray transients (Lasota 2001) might be able to accommodate such long quiescent episodes. We note that due to the very low peak fluxes during the 2002 outburst, we cannot rule out that, prior to the launch of *RXTE*, one or more outbursts occurred during the last four decades (i.e., since the birth of X-ray astronomy). Weak outbursts, such as the 2002 outburst of XTE J0929–314, could have easily been missed by X-ray satellites other than *RXTE*.

3.2.2. Constraints obtained when assuming mass transfer solely via gravitational radiation

Galloway et al. (2002) stated that if the mass transfer in XTE J0929–314 is driven by gravitational radiation then the time-averaged mass transfer rate \dot{M}_{GR} in this system should be

$$\dot{M}_{\text{GR}} = 5.5 \times 10^{-12} \left(\frac{M_{\text{ns}}}{1.4 M_{\odot}} \right)^{\frac{2}{3}} \left(\frac{M_{\text{c}}}{0.01 M_{\odot}} \right)^2 M_{\odot} \text{ yr}^{-1} \quad (3)$$

with M_{ns} the mass of the neutron star and M_{c} the mass of the companion star (both in solar masses). From the model by Brown et al. (1998; see also Rutledge et al. 2002) the quiescent luminosity L_{q} can be estimated via

$$L_{\text{q}} = 8.7 \times 10^{33} \left(\frac{\langle \dot{M} \rangle}{10^{-10} M_{\odot} \text{ yr}^{-1}} \right) \frac{Q}{1.45 \text{ MeV}} \text{ ergs s}^{-1} \quad (4)$$

with $\langle \dot{M} \rangle$ the time-averaged mass accretion rate onto the neutron star, and Q the amount of heat deposited in the crust per accreted nucleon (e.g., Haensel & Zdunik 1990). If we assume that the matter transfer from the companion star is solely driven by gravitational radiation and that all the matter transferred from the companion star is eventually accreted onto the neutron star then $\langle \dot{M} \rangle = \dot{M}_{\text{GR}}$. Substituting equation 3 in equation 4 gives

$$L_{\text{q}} = 4.8 \times 10^{32} \left(\frac{M_{\text{ns}}}{1.4 M_{\odot}} \right)^{\frac{2}{3}} \left(\frac{M_{\text{c}}}{0.01 M_{\odot}} \right)^2 \frac{Q}{1.45 \text{ MeV}} \text{ ergs s}^{-1} \quad (5)$$

If $M_{\text{ns}} = 1.4 M_{\odot}$, then Galloway et al. (2002) obtained a minimum mass for the companion star of $0.008 M_{\odot}$ (thus $M_{\text{c}} > 0.008 M_{\odot}$). If we further assume $Q = 1.45 \text{ MeV}$, then $L_{\text{q}} > 3 \times 10^{32} \text{ ergs s}^{-1}$. Only for large distances ($> 15 \text{ kpc}$) can the upper-limits on any contribution of a thermal component be consistent with this lower-limit on the quiescent luminosity (if M_{c} is not much greater than the minimum allowed value of $0.008 M_{\odot}$). For

smaller distances the predicted quiescent luminosity for a thermal component is a factor 2–8 times too high (this discrepancy becomes worse if M_c becomes larger). Firm conclusions can only be obtained when the exact luminosity of the thermal component can be measured with better data. However, our results already suggest that the quiescent luminosity predicted is higher than that measured if we assume that the matter transfer from the companion star is solely driven by gravitational radiation and that all the matter transferred is accreted onto the neutron star. Possible reasons for this discrepancy are that not all the matter transferred is accreted onto the neutron star or that enhanced cooling processes occur in the neutron-star core.

3.3. The non-detection of XTE J1751–305

Despite the fact that we could not conclusively detect XTE J1751–305 during our observation, the limits on the X-ray flux of this source can still be used to provide further insight into the quiescent emission of neutron star X-ray transients. We do not know the spectral shape of the quiescent emission of this system and therefore in § 2.2 we calculated the flux upper limits assuming two different spectral models (either a black-body or a power-law model; equations 1 and 2). The limits obtained using the black-body model are most useful for constraining the cooling neutron star model which assumes that the emission is due to thermal radiation from the neutron-star surface. We will attempt to constrain this model once again taking into account the limited observational knowledge about the time-averaged accretion rate of the source (§ 3.3.1) and assuming that the mass transfer is solely due to gravitational radiation and that all matter will eventually be accreted by the neutron star (§ 3.3.2). Here we first discuss the possibility that the source emitted a power-law shaped quiescent X-ray spectrum.

The two other accretion-driven millisecond X-ray pulsar which have been observed in quiescence have shown a power-law dominated quiescent X-ray spectrum with photon indices of 1.5 ± 0.3 (SAX J1808.4–3658; Campana et al. 2002) and 1.8 ± 0.6 (XTE J0929–314; Tab. 1). If we assume that XTE J1751–305 has also a power-law shaped quiescent spectrum, then, using equation 2, we get 0.5–10 keV flux upper limits on the quiescent emission of $2.5 - 3.5 \times 10^{-15}$ ergs s^{-1} cm^{-2} (assuming a range of 1–3 for the photon index, which covers the allowed values of the photon indices for SAX J1808.4–3658 and XTE J0929–314), giving 0.5–10 keV luminosity upper limits of $1.9 - 2.7 \times 10^{31} (\frac{d}{8 \text{ kpc}})^2$ ergs s^{-1} (d in kpc). If the distance toward XTE J1751–305 is < 11 kpc (thus the source is located in the Galactic center region) and the quiescent spectrum follows a power-law shape, then XTE J1751–305 would be the intrinsically faintest quiescent neutron-star X-ray transients so far known. However, if the

source is located at a larger distance, SAX J1808.4–3658 would still remain the faintest quiescent system (with a luminosity of $\sim 5 \times 10^{31}$ ergs s $^{-1}$; Campana et al. 2002), unless it can be confirmed that XTE J0929–314 can become at times fainter than SAX J1808.4–3658 (see § 3.1).

3.3.1. Constraints obtained when using the 2002 outburst fluence

According to Markwardt et al. (2002), the 2–200 keV fluence of the 2002 outburst of XTE J1751–305 was 2.5×10^{-3} ergs cm $^{-2}$. Since no bolometric correction factor is currently available, we will use this fluence, but we note that the bolometric fluence could be significantly higher (a factor of a few) and thus also the predicted quiescent thermal flux. Markwardt et al. (2002) found a previous outburst of the source in June 1998, resulting in a recurrence time of ~ 3.8 years. If this is the typical recurrence time of the source, then the time-averaged accretion rate will be $\langle F_{\text{acc}} \rangle \sim 2.1 \times 10^{-11}$ ergs s $^{-1}$ cm $^{-2}$. Since the predicted quiescent flux is given by $F_{\text{q}} = \frac{\langle F_{\text{acc}} \rangle}{135}$ (§ 3.2.1), this results in $F_{\text{q}} = 1.6 \times 10^{-13}$ erg s $^{-1}$ cm $^{-2}$, which is significantly larger than the maximum bolometric flux (2.7×10^{-14} ergs s $^{-1}$ cm $^{-2}$) we obtained for a possible thermally shaped quiescent spectrum. It might be possible that the average recurrence time of the source is larger than the 3.8 years found for the two outbursts so far observed. Using the method outlined in § 3.2.1, we find that the source must have typical quiescent episodes of > 22 years for the predicted quiescent flux to come down to the calculated flux limits. Such a recurrence time scale is not uncommon among the neutron-star X-ray transients. Another possibility for the discrepancy between the predicted quiescent flux and the limits on the actual flux is that the neutron star in XTE J1751–305 is colder than expected due to enhanced cooling in its core.

3.3.2. Constraints obtained when assuming mass transfer solely via gravitational radiation

Similar to XTE J0929–314, it also has been suggested for XTE J1751–305 (Markwardt et al. 2002) that the mass transfer might be due to gravitational radiation. If true, then \dot{M}_{GR} in this system should be (Markwardt et al. 2002)

$$\dot{M}_{\text{GR}} = 1.2 \times 10^{-11} \left(\frac{M_{\text{ns}}}{1.4 M_{\odot}} \right)^{\frac{2}{3}} \left(\frac{M_{\text{c}}}{0.0137 M_{\odot}} \right)^2 M_{\odot} \text{ yr}^{-1}. \quad (6)$$

If we assume that the matter transfer is solely driven by gravitational radiation and that all the matter is eventually accreted onto the neutron star then we can again set $\langle \dot{M} \rangle = \dot{M}_{\text{GR}}$.

Substituting equation 6 in equation 4 gives for the predicted quiescent luminosity (again assuming $Q = 1.45$ MeV)

$$L_q = 1.0 \times 10^{33} \left(\frac{M_{\text{ns}}}{1.4M_{\odot}} \right)^{\frac{2}{3}} \left(\frac{M_c}{0.0137M_{\odot}} \right)^2 \text{ ergs s}^{-1}. \quad (7)$$

Markwardt et al (2002) obtained a minimum mass for the companion star of $M_c > 0.0137 M_{\odot}$, when assuming a neutron star mass of $1.4 M_{\odot}$. Using these values for the masses of the companion and the neutron star, we find that the predicted quiescent luminosity is given by $L_q > 1 \times 10^{33} \text{ ergs s}^{-1}$. The 0.5–10 keV flux upper limit assuming a black body spectral model is given by equation 1. If $kT > 0.1$ keV (which is typically observed for other neutron star X-ray transients in their quiescent states), this gives a 0.5–10 keV luminosity upper limit of $> 2 \times 10^{32} \frac{d}{8 \text{ kpc}} \text{ ergs s}^{-1}$ (d in kpc). The bolometric luminosity limit could be a factor of a few larger. Only for relatively large distances ($> 10 - 15$ kpc; depending on the bolometric correction factor) can the measured upper limit on the luminosity become consistent with the predicted luminosity. For effective temperatures below 0.1 keV, the bolometric luminosity as calculated via $L_{\text{bol}} = 4\pi\sigma R^2 T_{\text{eff}}^4$ (with R and T the neutron star radius and surface temperature for an observer at infinity and σ the Stefan-Boltzmann constant) will become quite low and will not be consistent with the predicted luminosity. This indicates that the effective temperature cannot be too low in order to be consistent with the predicted quiescent luminosity.

3.4. Constraining the magnetic field of the neutron stars in XTE J0929–314 and XTE J1751–305

Recently, Burderi et al. (2002) and Di Salvo & Burderi (2003) constrained the magnetic field strengths of the neutron stars in several neutron-star X-ray transients (i.e., KS 1731–260, SAX J1808.4–3658 and Aql X-1) based on their measured quiescent luminosities and on the knowledge of the spin rate of their neutron stars⁸. To constrain the magnetic field strength, they used two proposed mechanisms which might produce X-rays in quiescence: *a*) residual accretion onto the neutron star at a very low accretion rate; *b*) neutron star rotational energy which is converted into radiation (a fraction of which might be released

⁸SAX J1808.4–3658 exhibits coherent oscillations in its persistent X-ray emission during outbursts which reflect the spin rate of the neutron star (Wijnands & van der Klis 1998). KS 1731–260 and Aql X-1 exhibit nearly-coherent oscillations during thermonuclear flashes on the neutron star surfaces (Smith, Morgan, & Bradt 1997; Zhang et al. 1998). Those oscillations are likely to be directly related to the neutron star spin rate as well (see, e.g., Strohmayer & Bildsten 2004 for a recent review).

in X-rays) because of the presence of a rotating magnetic dipole. They note that thermal emission from a cooling neutron star which is heated during outburst might also contribute to the quiescent X-ray emission and that the measured quiescent luminosities are therefore an upper limit on the X-ray contribution due to the above discussed scenarios.

They divided scenario *a* into two possibilities. The first (*a1*) assumes that the radius of the magnetosphere is inside the co-rotation radius and accretion onto the neutron star surface is possible; the second (*a2*) assumes that the magneto-spheric radius is outside the co-rotation radius but inside the radius of the light cylinder and accretion onto the neutron star is not possible but an X-ray emitting accretion disk might still exist with an inner radius larger than the co-rotation radius. Scenario *b* can also be divided into two possibilities. The first (*b1*) assumes that the X-ray emission in quiescence is due to reprocessing of part of the bolometric luminosity from the rotating neutron star into X-rays in the shock front between the pulsar wind and the circumstellar matter; the second (*b2*) assumes that the X-ray emission is intrinsic emission from the radio pulsar.

Following the method outlined by Burderi et al. (2002) and Di Salvo & Burderi (2003) and using the maximum quiescent luminosity from our fits ($1.2 \times 10^{32} (\frac{d}{10 \text{ kpc}})^2 \text{ ergs s}^{-1}$, with d in kpc) and the spin rate (185 Hz; Galloway et al. 2002) of XTE J0929–314, we found that the magnetic field strength of the neutron star in this system should be $< 2 \times 10^7 \frac{d}{10 \text{ kpc}} \text{ Gauss}$ (scenario *a1*), $< 3 \times 10^9 \frac{d}{10 \text{ kpc}} \text{ Gauss}$ (*a2*), $< 5 \times 10^8 \frac{d}{10 \text{ kpc}} \text{ Gauss}$ (*b1*), and $< 3 \times 10^9 (\frac{d}{10 \text{ kpc}})^{0.76} \text{ Gauss}$ (*b2*). Therefore, from these four scenarios the magnetic field strength of the neutron star in XTE J0929–314 can be constrained to be $< 3 \times 10^9 \frac{d}{10 \text{ kpc}} \text{ Gauss}$.

We also calculated the limits on the magnetic field strength of the neutron star in XTE J1751–305. The maximum flux limit of $2.7 \times 10^{-14} \text{ ergs s}^{-1} \text{ cm}^{-2}$ we obtained was for a spectral model which we assumed to be a simple black body shape, resulting in a luminosity limit of $2 \times 10^{32} \frac{d}{8 \text{ kpc}} \text{ ergs s}^{-1}$ (with d in kpc). Using the spin frequency of 435 Hz (Markwardt et al. 2002), this gives limits on the magnetic field strength of $< 1 \times 10^7 \frac{d}{8 \text{ kpc}} \text{ Gauss}$ (scenario *a1*), $< 5 \times 10^8 \frac{d}{8 \text{ kpc}} \text{ Gauss}$ (*a2*), $< 1 \times 10^8 \frac{d}{8 \text{ kpc}} \text{ Gauss}$ (*b1*), and $7 \times 10^8 \frac{d}{8 \text{ kpc}} \text{ Gauss}$ (*b2*). When assuming a power-law spectral model for the quiescent spectrum of XTE J1751–305, the upper limits on the fluxes are significantly smaller, with a maximum luminosity limit of $3 \times 10^{31} \frac{d}{8 \text{ kpc}}$ (with d in kpc), which would make the magnetic field limits a factor of > 2 less (the maximum upper limit would be again for scenario *b2* and is $< 3 \times 10^8 \frac{d}{8 \text{ kpc}} \text{ Gauss}$). Therefore, from these four scenarios the magnetic field strength of the neutron star in XTE J1751–305 can be constrained to be $< 3 - 7 \times 10^8 \frac{d}{8 \text{ kpc}} \text{ Gauss}$ (depending on assumed spectral model for the quiescent spectrum).

Although this method still has significant uncertainties (i.e., due to the lack of understanding of the structure of the accretion flow geometry in quiescent X-ray transients; see

Burderi et al. 2002 and Di Salvo & Burderi 2003 for a more detailed discussion), our limits on the magnetic field of the neutron stars in XTE J0929–314 and XTE J1751–305 are consistent with the expectation that these neutron stars have a low but non-negligible (since they exhibit pulsations during accretion outbursts) magnetic field strength.

We thank Peter Jonker for allowing us to use his *K*-band image of the region around XTE J1751–305 and for comments on an early version of this paper. We thank Jae Sub Hong for useful discussion about the quantile analysis method.

REFERENCES

Arnaud, K. 1996, in G. Jacoby & J. Barnes (eds.), *Astronomical Data Analysis Software and Systems V.*, Vol. 101, p. 17, ASP Conf. Series.

Asai, K., Dotani, T., Hoshi, R., Tanaka, Y., Robinson, C. R., & Terada, K. 1998, PASJ, 50, 611

Brown, E. F., Bildsten, L., & Rutledge, R. E. 1998, ApJ, 504, L95

Burderi, L. et al. 2002, ApJ, 574, 930

Cash, W. 1979, ApJ, 228, 939

Campana, S. & Stella, L. 2000, ApJ, 541, 849

Campana, S., Colpi, M., Mereghetti, S., Stella, L., Tavani, M. 1998, A&A Rev., 8, 279

Campana, S., et al. 2002, ApJ, 575, L15

Chen, W., Shrader, C. R., & Livio, M. 1997, ApJ, 491, 312

Di Salvo, T. & Burderi, L. 2003, A&A, 397, 723

Dotani, T., Asai, K., & Wijnands, R. 2000, ApJ, 543, L145

Galloway, D. K., Chakrabarty, D., Morgan, E. H., & Remillard, R. A. 2002, ApJ, 576, L137

Gehrels, N. 1986, ApJ, 303, 336

Greenhill, J. G., Giles, A. B., & Hill, K. M. 2002, IAU Circ., 7889

Haensel, P. & Zdunik J. L. 1990, A&A, 227, 431

Hong, J., Schlegel, E. M., & Grindlay, J. E. 2004, ApJ, in press (astro-ph/040646)

Jonker, P. G., et al. 2003, MNRAS, 344, 201

Jonker, P. G., Wijnands, R., & van der Klis, M. 2004a, MNRAS, 349, 94

Jonker, P. G., Galloway, D. K., McClintock, J. E., Buxton, M., Garcia, M., & Murray, S. 2004b, MNRAS, in press (astro-ph/0406208)

Juett, A. M., Galloway, D. K., & Chakrabarty, D. 2003, ApJ, 587, 754

Lasota, J.-P. 2001, NewA Rev., 45, 449

Maritz, J. S. & Jarrett, R. G. 1978, Journal of American Statistical Association, 73, 194

Markwardt, C.B & Swank, J. H. 2003, IAU Circ., 8144

Markwardt, C. B., Swank, J. H., Strohmayer, T. E., in 't Zand, J. J. M., & Marshall, F. E. 2002, ApJ, 575, L21

Markwardt, C. B., Smith, E., & Swank, J. H. 2003, IAU Circ.8080

Miller, J. M., et al. 2003, ApJ, 583, L99

Remillard, R. A. 2002, IAU Circ., 7888

Remillard, R. A., Swank, J., & Strohmayer, T. 2002, IAU Circ., 7893

Rutledge, R. E., Bildsten, L., Brown, E. F., Pavlov, G. G., & Zavlin, V. E., 2001, ApJ, 551, 921

Rutledge, R. E., Bildsten, L., Brown, E. F., Pavlov, G. G., Zavlin, V. E., Ushomirsky, G., 2002, ApJ, 580, 413

Rupen, M. P., Dhawan, V., & Mioduszewski, A. J. 2002, IAU Circ., 7893

Smith, D. A., Morgan, E. H., & Bradt, H. 1997, ApJ, 479, L137

Stella, L., Campana, S., Colpi, M., Mereghetti, S., & Tavani, M. 1994, ApJ, 423, L47

Stella, L., Campana, S., Mereghetti, S., Ricci, D., & Israel, G. L. 2000, ApJ, 537, L115

Strohmayer, T. & Bildsten, L. 2004, To appear in 'Compact Stellar X-ray Sources', eds. W. H. G. Lewin & M. van der Klis, Cambridge University Press (astro-ph/0301544)

Tomsick, J. A., Gelino, D. M., Halpern, J. P., & Kaaret, P. 2004, ApJ, 610, 933

Wijnands, R. & van der Klis, M. 1998, Nature, 394, 344

Wijnands, R., Miller, J. M., Markwardt, C., Lewin, W. H. G., van der Klis, M. 2001, ApJ, 560, L159

Wijnands, R. et al. 2004, ApJ, submitted (astro-ph/0310144)

Zhang, W., Jahoda, K., Kelley, R. L., Strohmayer, T. E., Swank, J. H., & Zhang, S. N. 1998, ApJ, 495, L9

Zavlin, V. E., Pavlov, G. G., & Shibanov, Yu. A., 1996, A&A, 315, 141

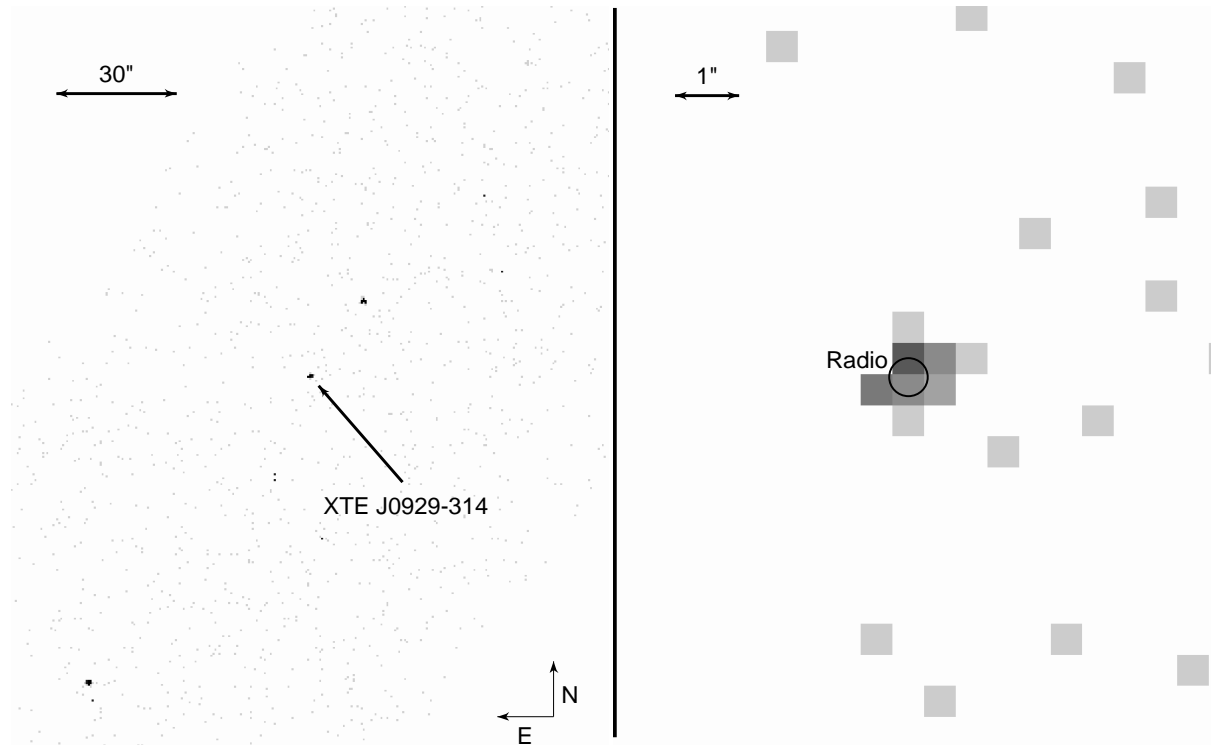


Fig. 1.— The *Chandra* image of the field around XTE J0929–314 (left) and a close-up of XTE J0929–314 (right) with the radio error circle for the source obtained during outburst (Rupen et al. 2002). In both figures, north is up and east is to the left. In the left panel the arrow indicates which source is XTE J0929–314. The source located to the north-west of XTE J0929–314 is CXOU J092919.1–312244 and the source to the south-east (in the bottom left corner) is CXOU J092924.4–312420.

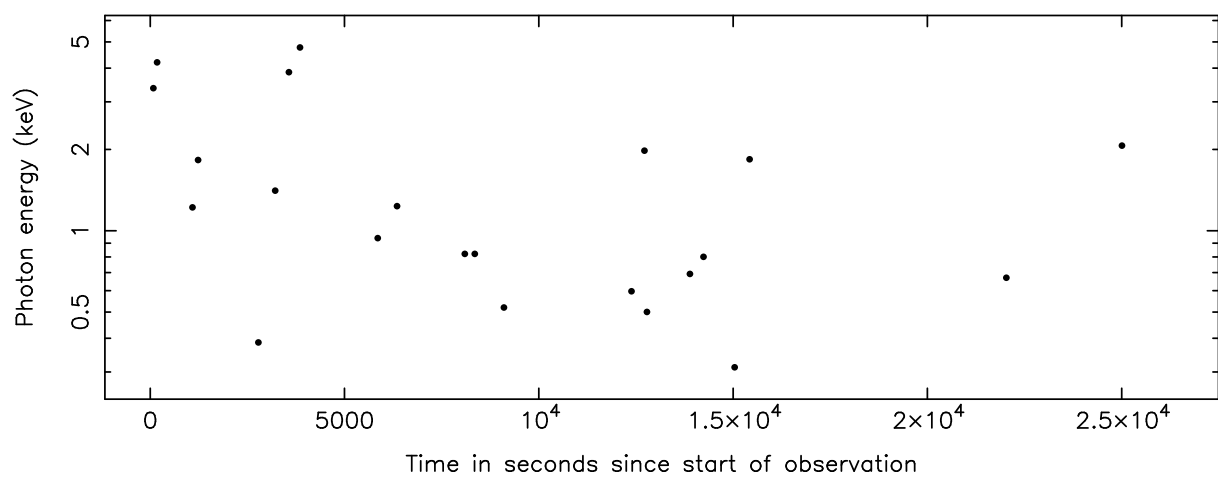


Fig. 2.— The energy of the detected photons versus the time of detection (since the start of the observation).

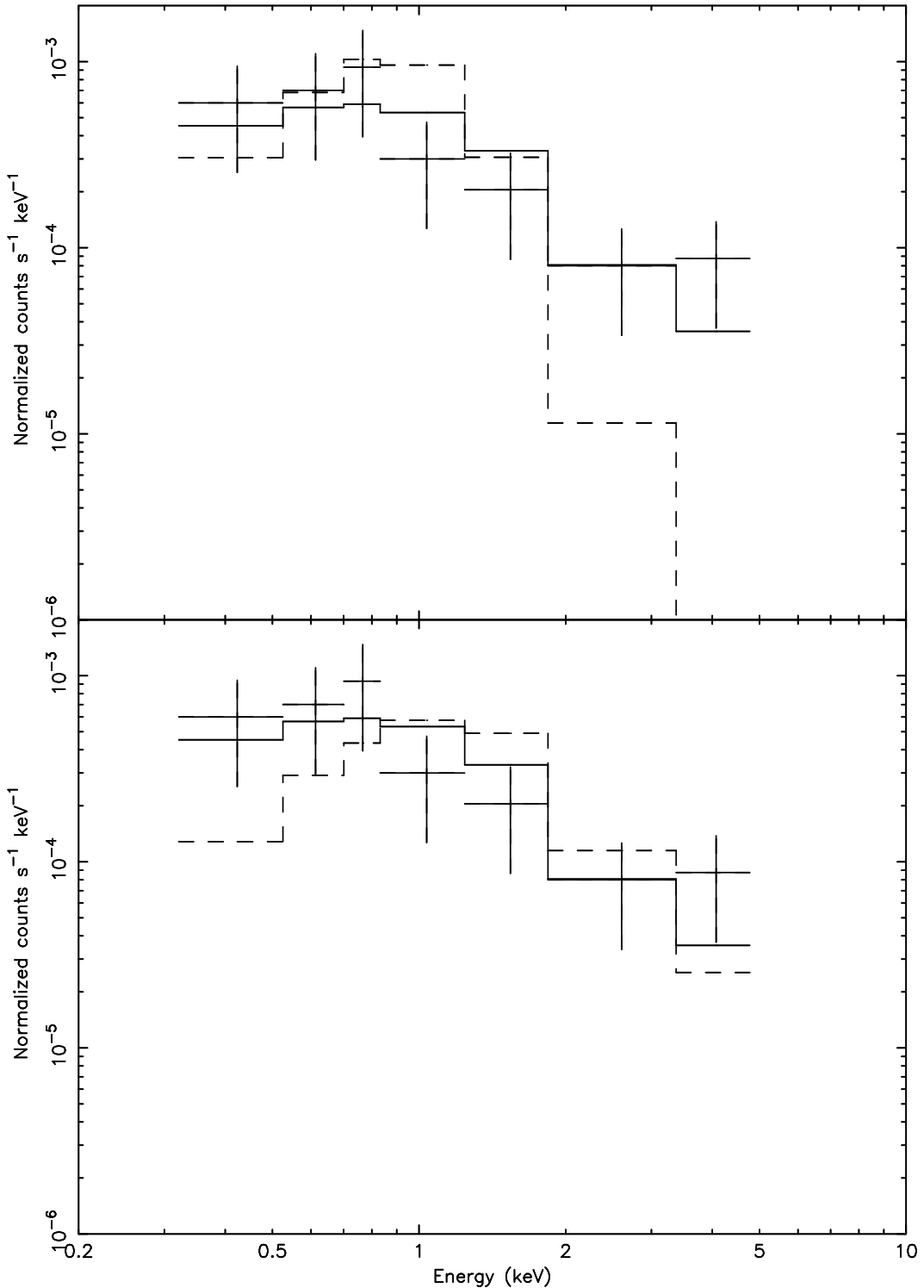


Fig. 3.— The time-averaged spectrum of XTE J0929–314. In the top panel, we show the best power-law fit to the data (solid line) and the best NSA fit through the data with a fixed normalization (to a distance of 10 kpc; dashed line). In the bottom panel, we again show the best power-law fit (solid line) but now the best NSA fit with the normalization left free (dashed line). For display purposes, the data were rebinned so that each bin has 3 counts but the spectra were fitted without any rebinning.

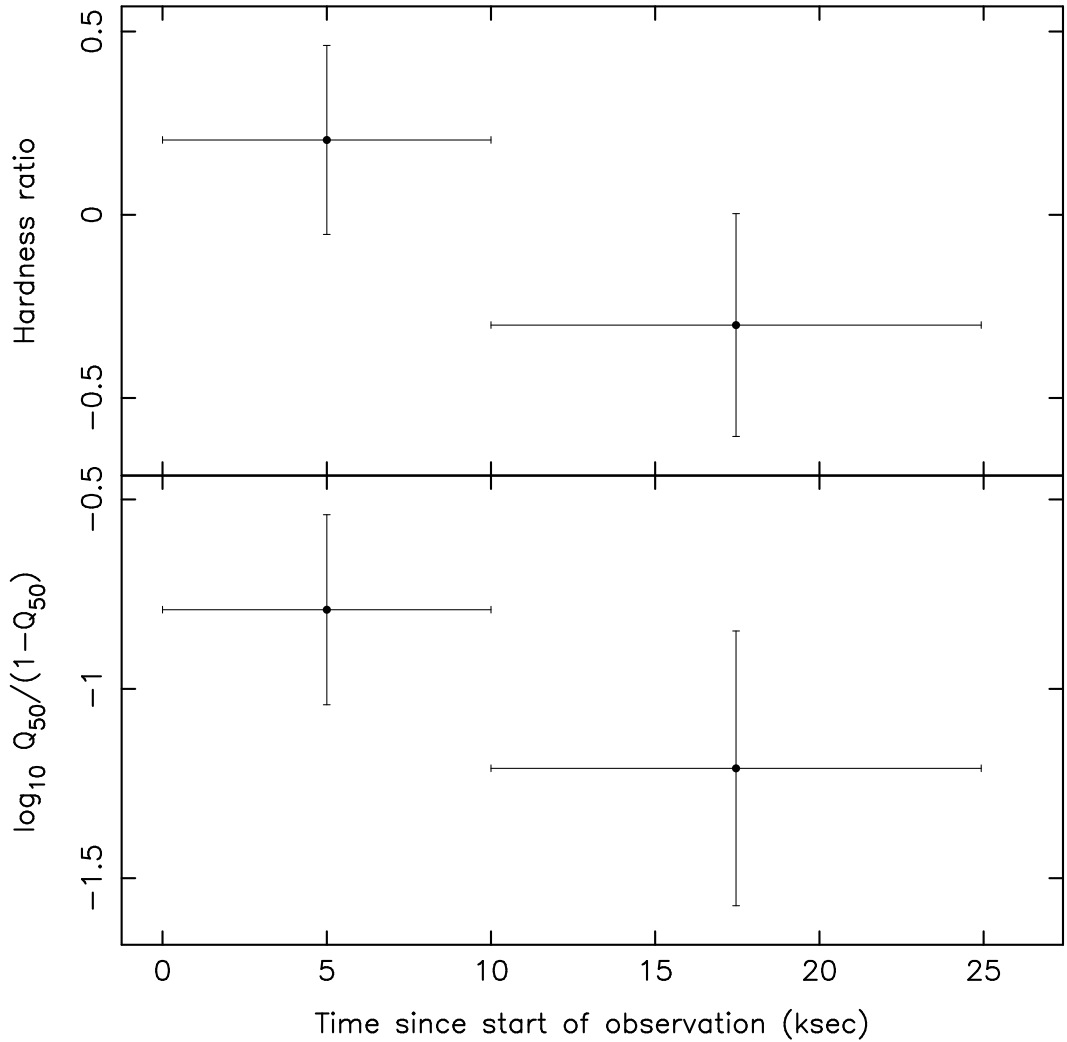


Fig. 4.— The hardness ratio (*top*) and the $\log_{10} \frac{Q_{50}}{1-Q_{50}}$ (*bottom*) versus the time during the observation. The hardness ratio is defined as the logarithm of the ratio between the number of photons detected with energies >1 keV and the number detected with energies <1 keV, and Q_{50} is the median quantile as defined by Hong et al. (2004).

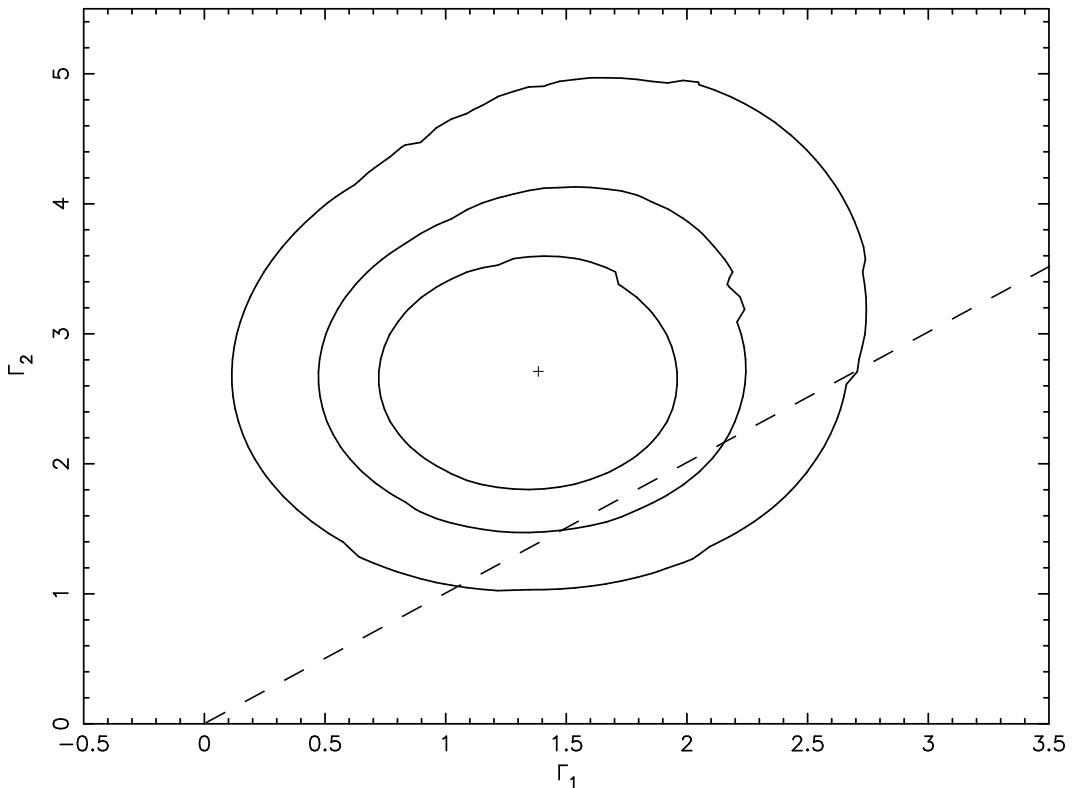


Fig. 5.— A comparison of the photon index of the first part of the data (0–10 ksec; Γ_1) with that of the second part of the data (the remaining \sim 14 ksec of the observation; Γ_2). The contours are the 68%, 90% and 99% confidence levels. The cross marks the position of the best-fit values of the indices. The dashed line indicates where both indices are equal.

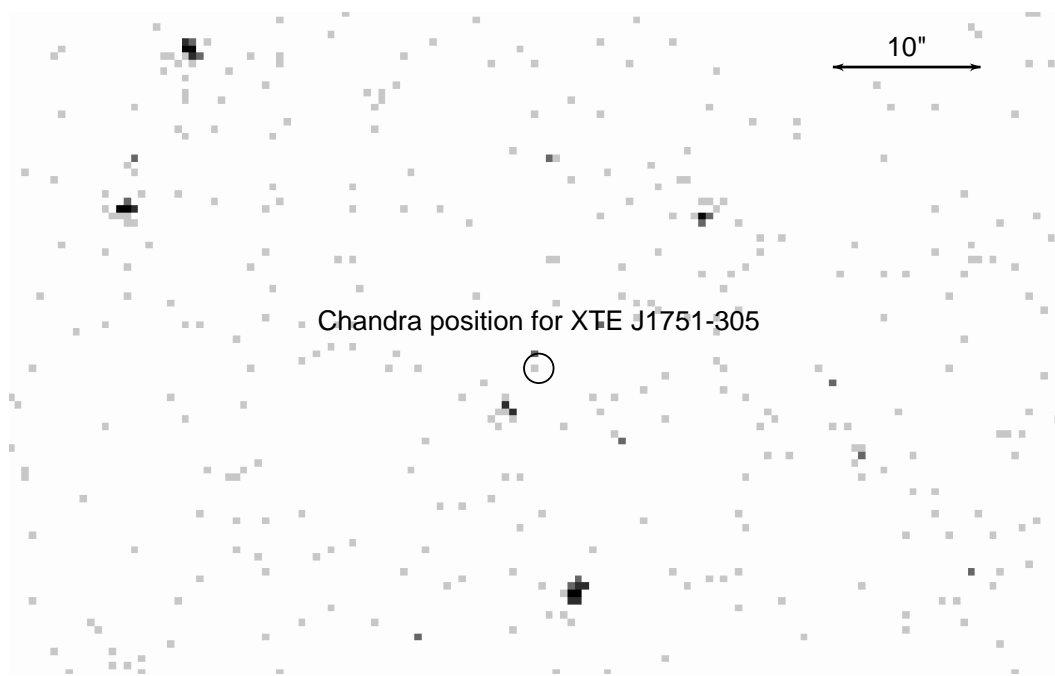


Fig. 6.— The 0.5–7 keV image of the region around XTE J1751–305. East is to the left and north is up. Several point sources are detected close to the position of XTE J1751–305 but none of these sources is consistent with the position of XTE J1751–305 (as indicated by the circle which has a radius of $1''$, which means that 90% of the energy of the photons is encircled in this region).

Table 1. Spectral fits of XTE J0929–314

Model ^a	N_{H} (10^{22} cm^{-2})	kT_{∞} (keV)	Γ	F^b ($10^{-15} \text{ ergs s}^{-1} \text{ cm}^{-2}$)	Fit quality ^c
NSA ($d = 5 \text{ kpc}$)	$0.3^{+0.2}_{-0.1}$	0.045 ± 0.005	—	9^{+7}_{-4}	1.00
NSA ($d = 10 \text{ kpc}$)	0.2 ± 0.2	$0.058^{+0.008}_{-0.009}$	—	9^{+9}_{-5}	1.00
NSA ($d = 15 \text{ kpc}$)	$0.2^{+0.2}_{-0.1}$	0.067 ± 0.08	—	9^{+7}_{-4}	1.00
Power-law	<0.06	—	$1.8^{+0.6}_{-0.5}$	6^{+4}_{-2}	0.68

^a For the neutron-star hydrogen atmosphere (NSA) model we used that of Zavlin et al. (1996) with a mass of $1.4 M_{\odot}$, a radius of 10 km, and a zero magnetic field strength for the neutron star in XTE J0929–314. The errors on the fit parameters are for 90% confidence levels.

^b The 0.5–10 keV unabsorbed flux.

^c The fit quality represents the fraction of 10,000 simulated spectra which have Cash-statistics better than that obtained for the actual data.

Table 2. Limits on any NSA contribution in XTE J0929–314^a

Distance d (kpc)	N_{H} (10^{22} cm $^{-2}$)	Γ	kT_{∞} (keV)	Bolometric luminosity ^b (10^{32} ergs s $^{-1}$)	Fraction in the power-law component ^c
5	<0.14	$1.2_{-1.1}^{+0.9}$	<0.04	<0.4	>0.77
10	<0.10	$1.1_{-1.2}^{+1.0}$	<0.05	<1.2	>0.70
15	<0.08	$1.1_{-1.3}^{+1.0}$	<0.05	<1.7	>0.78

^a Results of spectral fits assuming a NSA plus a power-law model. For the NSA model we used that of Zavlin et al. (1996) with a mass of $1.4 M_{\odot}$, a radius of 10 km, and a zero magnetic field strength for the neutron star in XTE J0929–314. The upper limits are for 90% confidence levels.

^b Bolometric luminosity of the neutron-star atmosphere component as seen by an observer at infinity

^c The minimum fraction of the 0.5–10 keV flux in the power-law component

Table 3. Possible spectral variability in XTE J0929–314

Time selection (ksec since start)	N_{H} (10^{22} cm^{-2})	Γ	Flux ^a ($10^{-15} \text{ ergs s}^{-1} \text{ cm}^{-2}$)	Fit quality
Separate fits				
0 – 10	<0.2	$1.3^{+0.9}_{-0.7}$	14^{+12}_{-4}	0.70
10 – end	<0.1	$2.6^{+1.2}_{-0.9}$	3^{+2}_{-1}	0.62
Simultaneous fits with tied N_{H}				
0 – 10	<0.07	1.3 ± 0.7	14^{+12}_{-6}	0.66
10 – end	“	$2.5^{+1.0}_{-0.9}$	3^{+2}_{-1}	“

^a The 0.5–10 keV unabsorbed flux